JVST A
Journal of Vacuum Science & Technology A

ARTICLE

avs.scitation.org/journal/jva

Molecular layer deposition of Nylon 2,6 polyamide polymer on flat and particle substrates in an isothermal enclosure containing a rotary reactor

Cite as: J. Vac. Sci. Technol. A 39, 052405 (2021); doi: 10.1116/6.0001162
Submitted: 21 May 2021 · Accepted: 22 July 2021 ·
Published Online: 11 August 2021

Tyler J. Myers and Steven M. George

AFFILIATIONS

Department of Chemistry, University of Colorado, Boulder, Colorado 80309

Note: This paper is part of the 2022 Special Topic Collection on Atomic Layer Deposition (ALD).

ABSTRACT

Polyamide thin films, designated Nylon 2,6, were grown on flat and particle substrates using molecular layer deposition (MLD) in a custom-built isothermal enclosure containing a rotary reactor. The polyamide films were grown using sequential exposures of ethylene diamine and adipoyl chloride. The reactor and precursors were contained in a fiberglass oven to keep all reactor components at the same temperature. A growth rate of 4.0 Å/cycle at 67 °C was determined on flat substrates with *ex situ* x-ray reflectivity and spectroscopic ellipsometry. The temperature dependence of the Nylon 2,6 displayed a peak growth rate at 67 °C with decreasing growth rates above and below this temperature. X-ray photoelectron spectroscopy of the polyamide film on flat substrates also revealed an elemental composition consistent with the Nylon 2,6 polymer with a small amount of chlorine in the film. The isothermal reactor allowed MLD to be performed consistently on high surface area particles at low temperatures. Transmission electron microscopy (TEM) images showed growth of the Nylon 2,6 films on ZrO_2, cellulose, and metformin particles that was consistent with the growth on witness wafers. The growth of the Nylon 2,6 films was also linear versus the number of MLD cycles. The TEM images displayed reproducible MLD growth on particles of varying size and composition. Fourier transform infrared spectroscopy and energy dispersive spectroscopy were consistent with the expected characteristics of the Nylon 2,6 polyamide film. Nylon 2,6 MLD should find application when low-temperature MLD is needed to coat thermally sensitive substrates such as organic films or pharmaceutical powders.

I. INTRODUCTION

Atomic layer deposition (ALD) is a powerful technique that uses sequential, self-limiting surface reactions to grow conformal, pinhole-free thin films with atomic layer control.[1] Gas-phase precursors are dosed consecutively resulting in stepwise growth of atomic layers after each surface reaction. Many inorganic materials have been deposited in this fashion, including oxides, nitrides, fluorides, and even single-element metals.[2] A similar approach known as molecular layer deposition (MLD) can be used to deposit polymer thin films.[3,4] MLD deposits entire molecular fragments during each reaction instead of growing the film by one atomic layer at a time.

Depending on the precursors, MLD can deposit all-organic or hybrid organic-inorganic films.[3,5] All-organic MLD is performed using homobifunctional precursors in the form A-X-A, where "A" is a chemical functional group and "X" is some organic fragment. The precursors are dosed sequentially, like ALD, and typically undergo condensation reactions. MLD has been used to deposit many types of organic polymers, including polyamides,[6–11] polyimide,[12] polyureas,[13,14] polyurethane,[15] polyester,[16] and polyimine.[4,17] MLD is an offshoot of an early gas-phase polymer growth technique known as vapor deposition polymerization (VDP).[18–20] VDP can be performed using sequential or alternating precursor exposures similar to MLD.[21–23]

MLD can also deposit hybrid organic-inorganic films.[3,5] These films are grown using an organic precursor and an inorganic precursor. Metal alkoxides are common organic-inorganic polymers. For example, alucone (aluminum alkoxide) is grown using ethylene glycol and trimethylaluminum.[24] Other metal alkoxides, known as metalcones, deposited with MLD include zincones,[25,26] zircones,[27] titanicones,[28] and hafnicones.[29]

Nanoengineering of particle surfaces has important industrial uses.[30] Many applications benefit from the ALD coating of nanoparticles.[31,32] Al_2O_3 ALD on BN nanoparticles was the first

demonstration of conformal, pinhole-free ALD films on high surface area nanoparticles.[33] Subsequently, a fluidized bed reactor was utilized for Al_2O_3 ALD on BN particles.[34] ALD of many other materials such as ZnO,[35,36] TiO_2,[37] ZrO_2,[38] and SnO_2[39] has also been demonstrated on high surface area nanoparticles. Further advances in particle ALD included ALD on alternate and complex structures like polymer particles[40] and carbon nanotubes.[41,42] ALD coatings on particles have also been used to increase the stability of Li ion battery electrodes,[43–45] quench photoactivity,[37] and improve catalytic processes.[46,47]

MLD has also been used to coat nanoparticles. Hybrid organic-inorganic MLD systems have commonly been used when depositing on particles.[48–50] The higher vapor pressure and robust reactivity of the inorganic precursors facilitates the growth of hybrid organic-inorganic MLD films. Silicon nanoparticle anodes were coated with alucone to improve mechanical strength during the lithiation process.[51] Other MLD systems create mesoporous or microporous films by calcination of the organic material of hybrid films to support separation, corrosion resistance, and catalytic applications.[52,53]

Despite advances in MLD systems, there are only a few demonstrations of the deposition of all-organic polymers on particle substrates.[54,55] The low vapor pressure of the precursors is one barrier for the MLD of all-organic polymers on particles. The low vapor pressure of the organic reactants can cause condensation on cold spots of the reactor and chemical vapor deposition (CVD) reactions resulting from slow purging of the organic precursors. Providing enough reactants to complete the reaction can also be difficult because mass transport is limited by the low vapor pressure of the organic precursor. Aggregation of particles during the MLD process can also be a problem. Together, these obstacles make coating high surface area particles with all-organic polymers a challenge.

Enclosing the MLD reactor inside of an isothermal oven can help solve some of these problems. Maintaining the reactor components and precursor sources at the same temperature prevents cold spots. This approach has been employed previously in a "spatial" MLD system.[8] A rotary reactor can help achieve fluidization of powders during the MLD process.[56–58] In this article, a custom-built isothermal enclosure containing a rotary reactor was used to investigate the growth of a polyamide designated Nylon 2,6 using the sequential reactions of ethylene diamine (ED) and adipoyl chloride (AC) on flat and particle substrates. An earlier report incorrectly designated this polyamide as Nylon 6,2.[11] The first number should reveal the number of carbons in the diamine. The second number should indicate the number of carbons in the dicarboxylic acid chloride. The growth, composition, and consistency of the Nylon 2,6 MLD process on both flat and particle substrates were explored at temperatures below 100 °C.

All-organic MLD systems can be deposited on particles for many applications. One use is as a coating on pharmaceutical powders to control the dissolution profile of the active ingredient.[55] MLD can also deposit organic films on polymer particles to functionalize their surface and impart stability and chemical resistance. These organic particles may be thermally sensitive and must be coated well below their decomposition and glass transition temperatures. At elevated temperatures, even as low as 80 °C, transitions from amorphous to crystalline or from one polymorph to another can have negative effects on drug solubility, bioavailability, and performance.[59] By performing the MLD process in an isothermal system, thermally sensitive substrates can be coated with all-organic thin films at relatively low temperatures.

II. EXPERIMENT

A. Isothermal reactor design

Experiments were performed in a custom-built enclosure containing a rotary reactor optimized for performing all-organic MLD on flat or particle substrates. Rotary reactors for performing ALD on particles have been reported previously.[56–58] Powders were housed in a stainless steel cylinder mounted onto a magnetic feedthrough (UHV Transfer Systems) and introduced into the chamber on-axis through a 2.75″ Conflat flange.

Figure 1(a) shows a cross section of the reactor showing the rotating mounted canister attached to the feedthrough. The reactor is set at a 7° angle to help keep powder inside the canister without having the sample congregate in the back.[57] Flat witness wafers

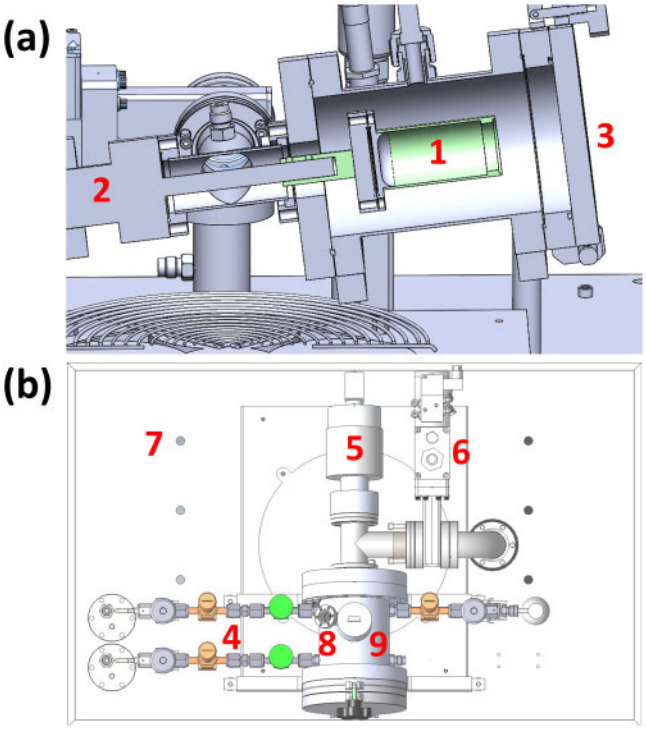

FIG. 1. (a) Cross section of a rotary reactor showing (1) particle canister attached to (2) magnetic feedthrough inside a reactor chamber. Particles are loaded through (3) quick access door. (b) Overhead view showing (4) precursor lines, external components of (5) magnetic feedthrough, and (6) gate valve. The base also has (7) larger openings to allow plumbing of high vapor pressure reactants for placement outside a heated enclosure. The reactor also contains (8) ConFlat port for an insertable thermocouple probe to measure temperature and (9) a capacitance manometer to monitor the pressure inside the chamber.

were also coated with MLD films inside this reactor. The witness wafers were placed in the reactor on a small stainless steel boat.

In the magnetic feedthrough, an outer set of high-temperature compatible SmCo magnets is coupled to a motor via gears and a belt. Rotation of the outer magnets rotates a set of magnets inside the feedthrough. This rotates a shaft that, in turn, rotates the mounted canister and agitates the powders inside the canister. A "laundry dryerlike" motion is desired where powders fall from the top of the canister in a continuous, cascading fashion.[56]

There are some differences implemented into the rotary reactor design to perform all-organic MLD on particles. Additional perturbation is achieved by installing an insertable scraper onto the inner wall of the front flange of the chamber. The point sits 0.5 mm from the top of the powder canister and knocks loose any powder stuck to the canister wall. The cylinder holding the particles is open-ended to prevent conductance limitations when dosing and purging low vapor pressure organic precursors.[57] Hardware includes two sizes of canisters to hold the powders: one small canister for research-scale experiments and one large canister for scale-up depositions. The small canister has a total volume of 19 cm^3 with a typical maximum powder capacity of 1 cm^3. The large canister has a total volume of 76 cm^3 with a typical maximum powder capacity of 4 cm^3.

Figure 1(b) shows an overhead view of the main reactor components. The reactor chamber has a low volume of ~1 l. In addition, short, direct precursor dosing modules maximize transport of the low vapor pressure reactants. One connection is left open to be occupied by the purge gas. An MKS gate valve is used for isolating the chamber from vacuum for static dosing. The reactor also features a ¼″ conductance-limiting exhaust pathway (not shown) that bypasses the gate valve for slow initial evacuation to avoid disturbing powders during the pressure decrease from atmosphere to vacuum. A 1.33″ Conflat port provides entry for an insertable thermocouple probe to measure the temperature inside the chamber. Pressure is monitored using a capacitance manometer on the top of the main reactor.

Reactor components and organic precursors are contained in a 32″ × 20″ × 28″ oven insulated with a 1″ thick fiberglass to create an isothermal environment. An isothermal environment is key when using a low vapor pressure precursor to maximize the use of vapor draw dosing and eliminate cold spots. A similar approach has been reported previously.[8] Figure 2 shows the rotary reactor enclosed in the oven where the translucent gray area represents the normally opaque enclosure. K-type thermocouples inside the oven, inside the reactor, and on reactor components monitor the temperature and show temperature variation of only 1–2 °C. Two handles (not shown) are attached to either side of the oven for removal.

The oven is heated by two 500 W finned strip heaters (Vulcan) powered by a Eurotherm 2048 Controller and Relay. A fan blade underneath the reactor pulls air in over the heaters and directs the air up through the center of the oven and over the reactor to ensure even heating of the entire volume. Tubing and

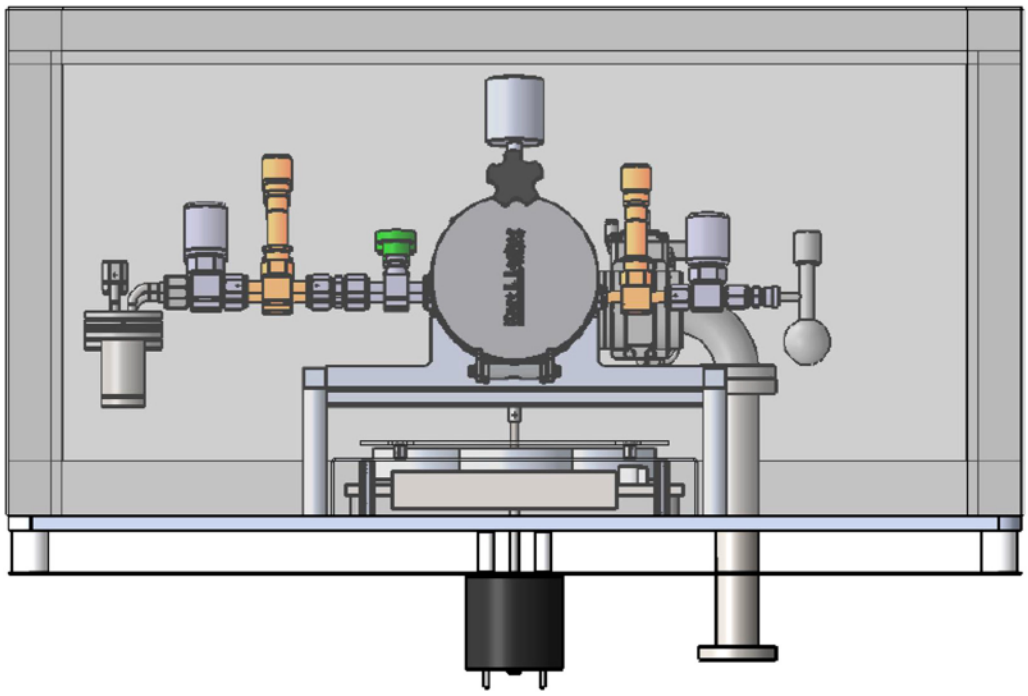

FIG. 2. Front view of an isothermal rotary reactor. The shaded gray area depicts an insulated fiberglass enclosure that maintains isothermal conditions inside the enclosure.

wiring for pneumatic actuation, pumping, heating and pressure, and temperature monitoring feed through the bottom of an insulated base. The reactor sits on this insulated base. The base also has larger openings to allow plumbing of high vapor pressure reactants that need to be placed outside the heated enclosure.

B. Nylon 2,6 polyamide reaction chemistry

Two reactants (Millipore Sigma), ethylene diamine (ED) and adipoyl chloride (AC), were used to perform the MLD of Nylon 2,6.[11] ED and AC are both liquids with vapor pressures of approximately 20 and 2 Torr at room temperature, respectively. The proposed surface reactions are as follows where an asterisk denotes a surface species:

$$\text{A)}\ -NH_2^* + ClCO(CH_2)_4COCl \rightarrow -NH-CO(CH_2)_4COCl^* + HCl, \quad (1)$$

$$\text{B)}\ -NH-CO(CH_2)_4COCl^* + H_2N(CH_2)_2NH_2 \rightarrow -NH-CO(CH_2)_4CO-NH(CH_2)_2NH_2^* + HCl. \quad (2)$$

Figure 3 shows the Nylon 2,6 MLD process and the reaction by-products. The initial AC exposure reacts with the amine group to release HCl, create an amide linkage, and add a molecule of adipoyl chloride minus a chlorine on the surface. This reaction also produces an acid chloride group. The amine of the subsequent ED exposure reacts with the acid chloride group to release hydrochloric acid and create another amide linkage. The Nylon 2,6 polymer was deposited using alternating exposures of AC and ED in a n[AB] fashion.

AC and ED precursors were contained in UltraTorr glass and stainless steel bubblers, respectively, and introduced into the chamber using vapor draw. The temperature of the precursors was determined by the temperature of the oven. Typical dose pressures were between 0.5 and 1 Torr. Deposition temperatures ranged from 50 to 90 °C. Low temperatures allow deposition on thermally sensitive materials like pharmaceutical powders.

Prior to the experiments, 100–200 mg of powder was added to the stainless steel canister and oven dried at 100 °C for 1 h. The canister was then loaded into the chamber and rotated at a speed of 10–50 rpm depending on the powder composition. Typical rotation speeds were 45 rpm (ZrO_2), 30 rpm (metformin), and 15 rpm (avicel). The chamber was evacuated to a pressure of 30 mTorr and the system was allowed to reach the equilibrium temperature for 2 h. The experiments were conducted after the internal chamber temperature and the oven temperature reached the same temperature.

Due to the high surface area of the powders, precursor exposures were static to ensure reaction with all surface sites. Typical exposure times were between 30 and 60 s. Following the precursor exposure, the system was pumped for 1 min. A N_2 gas purge was performed following this pumping. This N_2 purge consisted of 7 Torr of N_2 gas held statically in the chamber for 10 s and then opened to vacuum for 90 s. Each purge sequence consisted of 7 cycles of this process. During this time, the chamber and all dosing module lines were purged and evacuated to avoid condensation in the precursor lines. The results were obtained using precursor dose pressures of 1 Torr for 60 s.

C. Substrates and sample characterization

Flat substrates and high surface area powders were used to evaluate the Nylon 2,6 MLD process. Flat ZrO_2 ALD films on silicon coupons with an area of 1 cm^2 were used for the growth rate investigations. MLD film thicknesses were measured on the ZrO_2 films using a Bede D1 x-ray reflectometer (XRR) and a Woolam M-2000 spectroscopic ellipsometer (SE). A PHI 5600 x-ray photoelectron spectrophotometer with a monochromatized Al Kα x-ray source was used to determine film compositions and atomic percentages.

High surface area particle samples were ZrO_2 powders with a diameter of ~20 nm (99.5%, U.S. Research Nanomaterials), cellulose

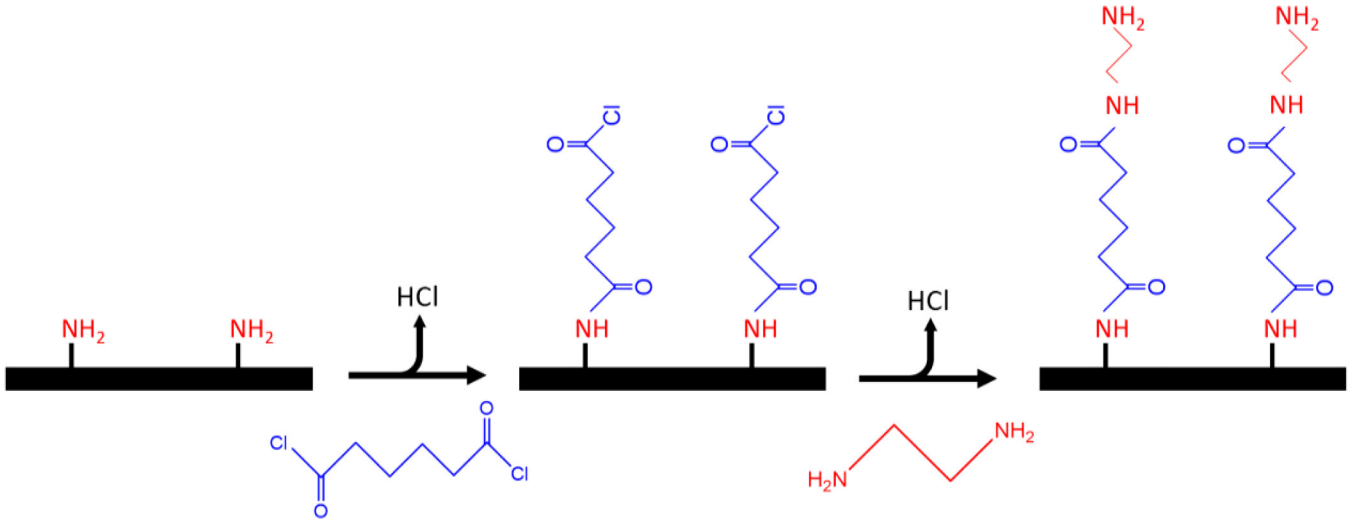

FIG. 3. Reaction schematic for Nylon 2,6 MLD using sequential exposures of adipoyl chloride and ethylene diamine.

polymer micropowders ($T_g \sim 133\,°C$) with a diameter of $\sim 200\,\mu m$, and metformin particles with a diameter of $\sim 45\,\mu m$ supplied from an industry partner. Coatable surface areas for each powder were approximately 5.3×10^4, 100, and 103 cm^2 for ZrO_2, cellulose, and metformin, respectively. Bulk and surface features of the film on ZrO_2 powder were monitored using a Nicolet 670 FITR spectrometer. The coated ZrO_2 powder with a surface area of >500 cm^2 was pressed into a tungsten grid for the transmission FTIR measurements. Images of coated powders were obtained using an FEI Tecnai T12 Spirit Transmission Electron Microscope (TEM). Instrumentation at EAG Laboratories was used for FIB-cut cross-section images and energy-dispersive mapping capabilities.

III. RESULTS AND DISCUSSION

A. Nylon 2,6 MLD growth and characterization on ZrO_2 wafers

Figure 4 shows the thickness of the Nylon 2,6 film on ZrO_2 witness wafers as determined by XRR and SE versus the number of MLD cycles at 57, 67, and 90 °C. At 67 °C, the polyamide film grows linearly at a rate of 4.0 Å/cycle. This behavior suggests that the polyamide film nucleates well on the substrate and the thickness can be controlled with the MLD process. This growth rate is similar to the growth rate of other polyamides deposited using MLD.[6–8,10,11] These comparable growth rates were observed at higher temperatures.

A growth rate of 4.0 Å/cycle is lower than the expected monolayer thickness of 13 Å for a Nylon 2,6 subunit in a polymer chain that is perpendicular to the surface. A maximum growth rate of 13 Å/cycle would be achieved if AC and ED exposures reacted and grew with linear chains perpendicular to the surface. Bond rotation and reactions that are not perpendicular to the surface could result in a lower growth rate. Many MLD systems exhibit this behavior. Several investigations explained low MLD growth rates in terms of polymer chains growing more parallel to the surface and resembling a "tangled pile of pasta."[6,7]

The isothermal environment helps prevent CVD and controls the MLD growth. Earlier MLD growth of Nylon 6,6 revealed growth rates higher than the expected chain length of the polyamide.[7] This behavior was attributed to Nylon 6,6 CVD reactions resulting in a growth rate per cycle outside the self-limiting regime. In this study, maintaining a constant temperature between organic precursors and reactor components helps eliminate cold spots and possible CVD reactions.

The Nylon 2,6 polyamide growth is linear at various temperatures. However, the growth rate decreases above and below 67 °C. The growth rates at 57 and 90 °C are 1.6 and 1.3 Å/cycle, respectively. Figure 5 shows the temperature dependence of the growth rate for the Nylon 2,6 film. The growth rate peaks at a temperature of 67 °C and then decreases at higher or lower temperatures. Attempts to deposit Nylon 2,6 films at temperatures below 50 °C were unsuccessful. XRR measurements did not show any Nylon 2,6 film present at these temperatures.

Previously demonstrated MLD systems have displayed an inverse temperature dependence where the growth rate decreases as the temperature increases.[6,7,24,26–29] This dependence has been attributed to more double reactions and the shorter residence time for precursors absorbed in the film at higher temperatures.[26,27,60] Many of the studies for the all-organic MLD systems did not investigate lower temperatures due to the long purge times necessary when using low vapor pressure organic precursors. Therefore, previous studies may not have accessed lower temperatures where the

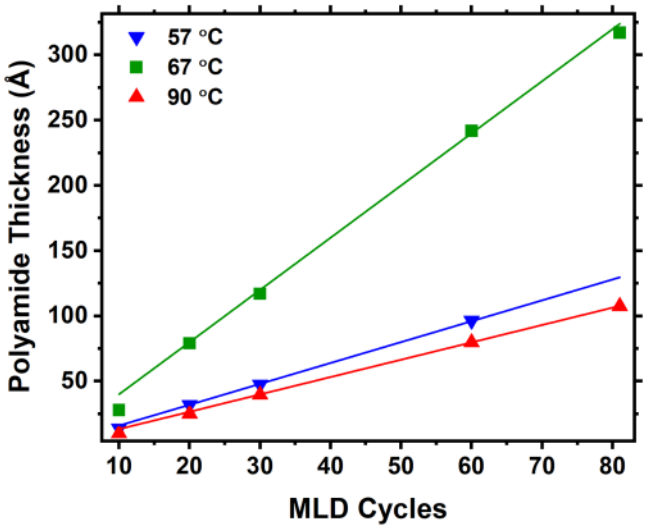

FIG. 4. Nylon 2,6 film thickness vs the number of MLD cycles at 57, 67, and 90 °C grown on ZrO_2 witness wafers. Thicknesses were obtained using x-ray reflectivity and spectroscopic ellipsometry measurements.

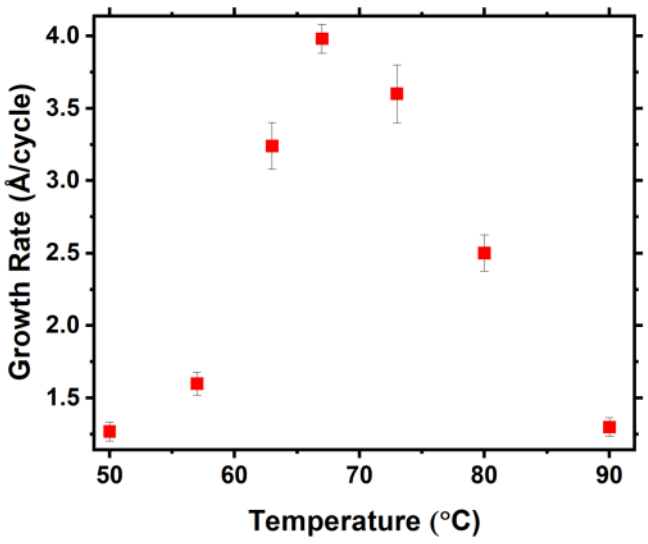

FIG. 5. Temperature dependence of Nylon 2,6 MLD growth rate using adipoyl chloride and ethylene diamine.

thermal activation barrier of the reaction may control the temperature dependence. At 67 °C, there may be a balance between thermochemically favorable reactions and residence times. The static deposition process may also accentuate this temperature dependence by allowing reactants ample time for absorption at lower temperatures.

An XPS survey scan was performed for a Nylon 2,6 MLD film with a thickness of 24 nm on a ZrO_2 witness wafer deposited at 67 °C to determine the film composition. Figure 6 shows the detected peak intensities versus binding energy after slight sputtering of the Nylon 2,6 film. High-intensity peaks at 285.0, 398.4, and 531.8 eV are observed that are attributed to C 1s, N 1s, and O 1s, respectively. Expected atomic percentages for a Nylon 2,6 film would be 16.7 at. % nitrogen, 16.7 at. % oxygen composition, and 66.7 at. % carbon. In comparison, the measured composition of the film is 12.2 at. % nitrogen, 15.1 at. % oxygen, and 70.8 at. % carbon. There is good agreement between the expectations and the measurements. The extra carbon is attributed to adventitious carbon resulting from sample transfer from the reactor to the *ex situ* XPS tool.

There are also two small peaks at 198.7 and 270.0 eV in Fig. 6. These peaks are assigned to Cl 2p and Cl 2s, respectively. Analysis quantifies this chlorine concentration at 1.3 at. %. Some chlorine can be explained by polymer chains terminated by Cl after adipoyl chloride exposures. Some chains in the film may not be easily accessible for reaction with the next precursor ED exposure. If the ED molecule cannot reach the end of the chain and react to form the amide linkage, the chain would remain terminated by chlorine.

Chlorine incorporation can also be explained by the static dosing. The reactants are exposed for 1 min during each reactant exposure. There is ample time for the reaction to go to completion but also time for the diffusion of the precursors into the film. The diffusion of reactants into polymers during ALD and MLD has been reported in the past.[60,61] The diffusion of unreacted AC precursors into the polyamide film would result in increased chlorine concentration. Purging can remove some of the diffused precursors but may not clear all unreacted precursors from the polymer film. Additional AC in the polymer film could also explain the slightly higher O at. % from the XPS analysis.

Additional chlorine in the polymer film could also result from a reaction of the HCl by-product with other components of the polyamide or the other reactants. Earlier studies of Nylon 6,6 MLD observed the reaction of HCl with the diamine precursor resulting in ammonium chloride salts.[7] This work uses similar polyamide precursors and there is a possibility for chloride salt formation. Static exposures can exaggerate this formation as the HCl by-product is not purged from the chamber until after the completion of the reactant exposure.

B. Nylon 2,6 MLD growth and characterization on particle substrates

Nylon 2,6 films were deposited on different particle substrates to demonstrate the feasibility of performing MLD on high surface area samples. Figure 7 displays a TEM image of a Nylon 2,6 film on ZrO_2 nanoparticles after 60 cycles of MLD at 67 °C. Sixty cycles at 67 °C should produce a 24 nm-thick film based on the 4.0 Å/cycle growth rate measured on witness wafers. The Nylon 2,6

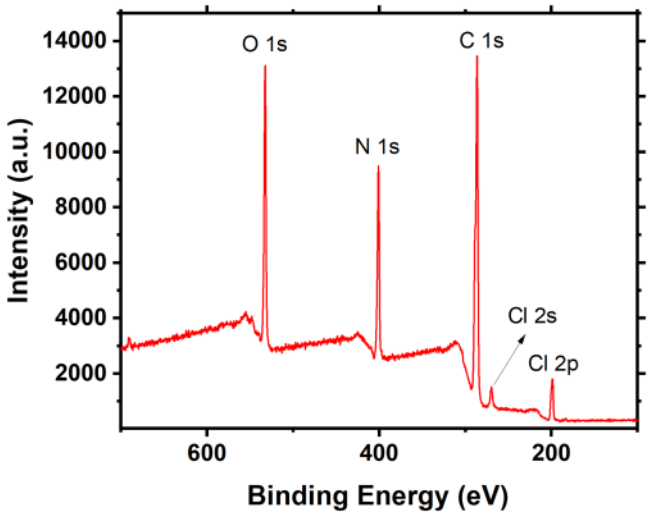

FIG. 6. XPS spectrum showing peak intensity vs binding energy for a Nylon 2,6 film grown on a ZrO_2 witness wafer. Elemental atomic percentages from the XPS peak intensities are consistent with the composition of Nylon 2,6 polymer.

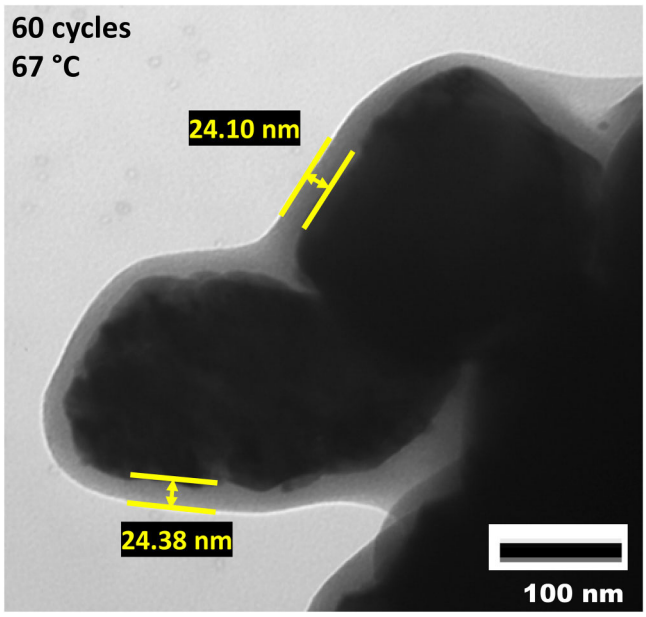

FIG. 7. TEM image of a ZrO_2 nanoparticle agglomerate after 60 cycles of Nylon 2,6 MLD at 67 °C. The film thickness is ~24 nm and consistent with a 4.0 Å/cycle growth rate measured on flat substrates.

film thickness measures between 23 and 25 nm. The film is mostly conformal around the edges of the nanoparticle agglomerate. Thicker films are observed in conductance-limited areas of the agglomerate. Increased purging and particle agitation may limit these thicker films. The polyamide film coats the entire nanoparticle agglomerate.

The film thickness on the particles can also be linearly tuned by varying the number of MLD cycles. Figure 8 shows TEM images of the edges of ZrO_2 nanoparticles coated with (a) 10 and (b) 30 cycles of Nylon 2,6 MLD at 67 °C. The Nylon 2,6 MLD film grows thicker with an increasing number of MLD cycles. The film thicknesses are consistent with the observed linear growth rate of 4.0 Å/cycle on witness wafers. The expected MLD thicknesses would be 4 and 12 nm for 10 and 30 MLD cycles, respectively. In comparison, the measured MLD thicknesses are 3.9 and 11.8 nm for 10 and 30 MLD cycles, respectively.

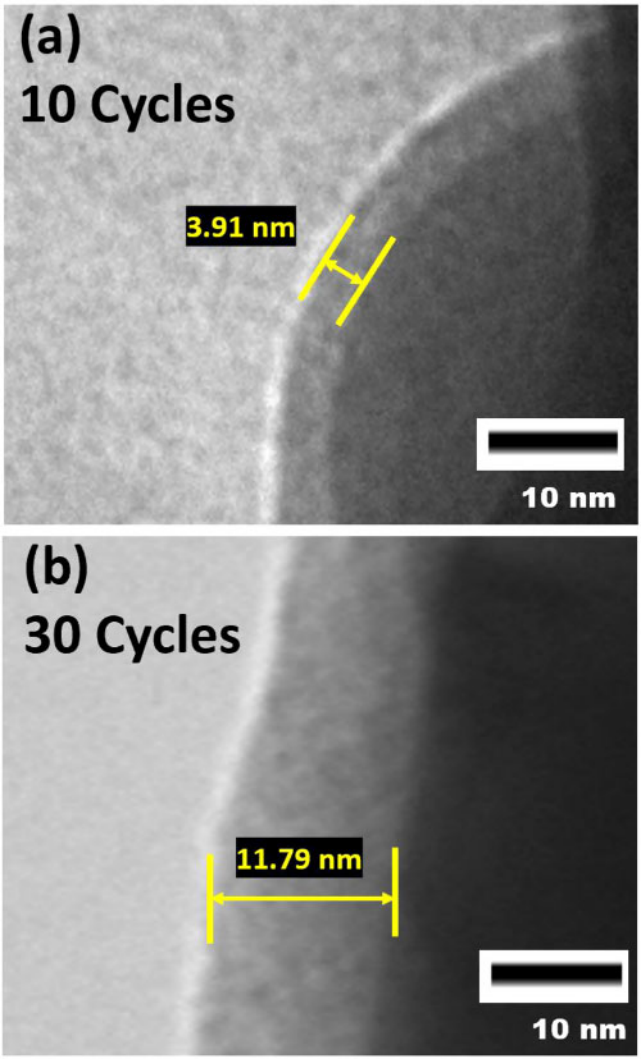

FIG. 8. TEM showing Nylon 2,6 film grown on ZrO_2 nanoparticles after (a) 10 cycles and (b) 30 cycles of MLD at 67 °C. The Nylon 2,6 film thickness increases from 3.9 nm after 10 cycles to 11.8 nm after 30 cycles.

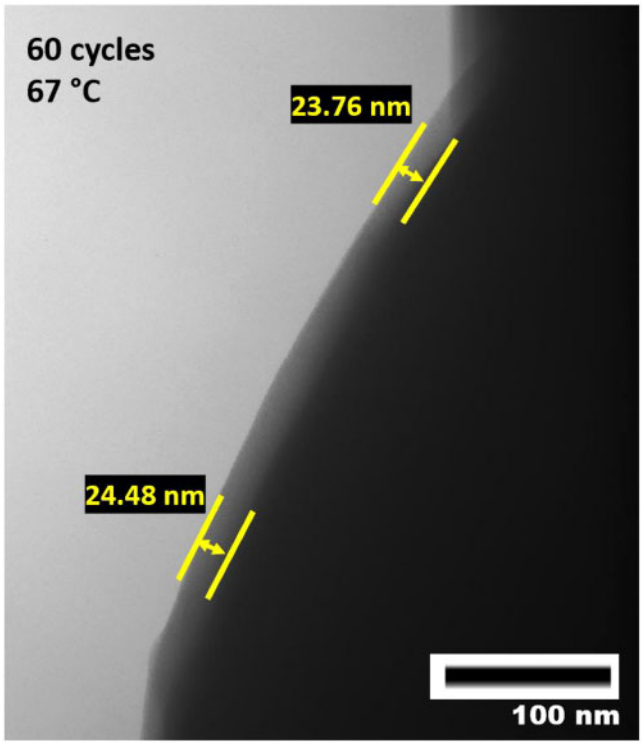

FIG. 9. TEM image of cellulose polymer micropowder after 60 cycles of Nylon 2,6 MLD at 67 °C. The film thickness of 23–25 nm is consistent with a 4.0 Å/cycle growth rate measured on flat substrates.

Nylon 2,6 MLD also performs well on particles of different compositions and sizes. Figure 9 shows 60 cycles of polyamide MLD at 67 °C on a large cellulose polymer particle with a diameter of ~200 μm. The TEM image shows a smooth and conformal film along the edge of the particle. The film thickness of 24–26 nm is consistent with XRR and SE measurements on witness wafers. The Nylon 2,6 MLD has been consistent for particles with over four orders of magnitude difference in size. The larger particles generally show better film conformality because of a lower tendency to agglomerate.

The consistency and versatility of Nylon 2,6 are also observed when coating a thermally sensitive pharmaceutical powder. Figure 10 depicts a metformin particle coated with 60 cycles of Nylon 2,6 MLD at 67 °C. Metformin is an active pharmaceutical ingredient used to treat type I diabetes. The metformin particles used in this study had an average particle size of 45 μm. The film thickness of 23.8 nm in Fig. 10 is consistent with XRR and SE measurements on witness wafers. The Nylon 2,6 MLD conformally coats the entire metformin particle.

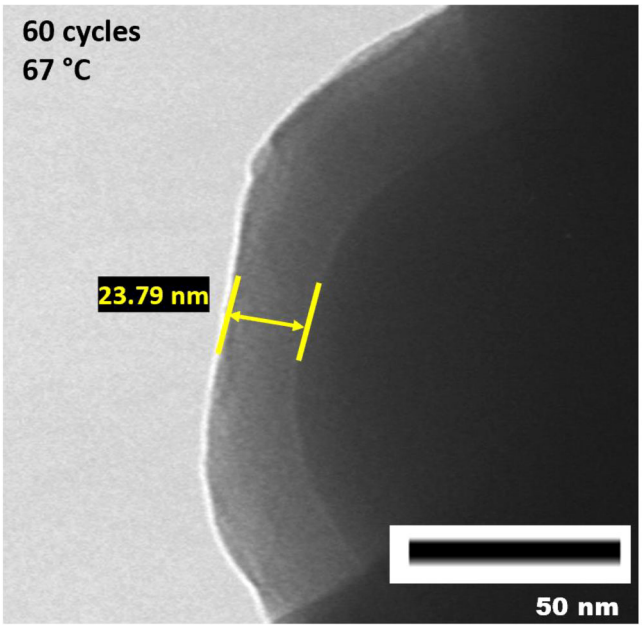

FIG. 10. TEM image of metformin after 60 cycles of Nylon 2,6 MLD at 67 °C. The film thickness of 23.8 nm is consistent with a 4.0 Å/cycle growth rate measured on flat substrates.

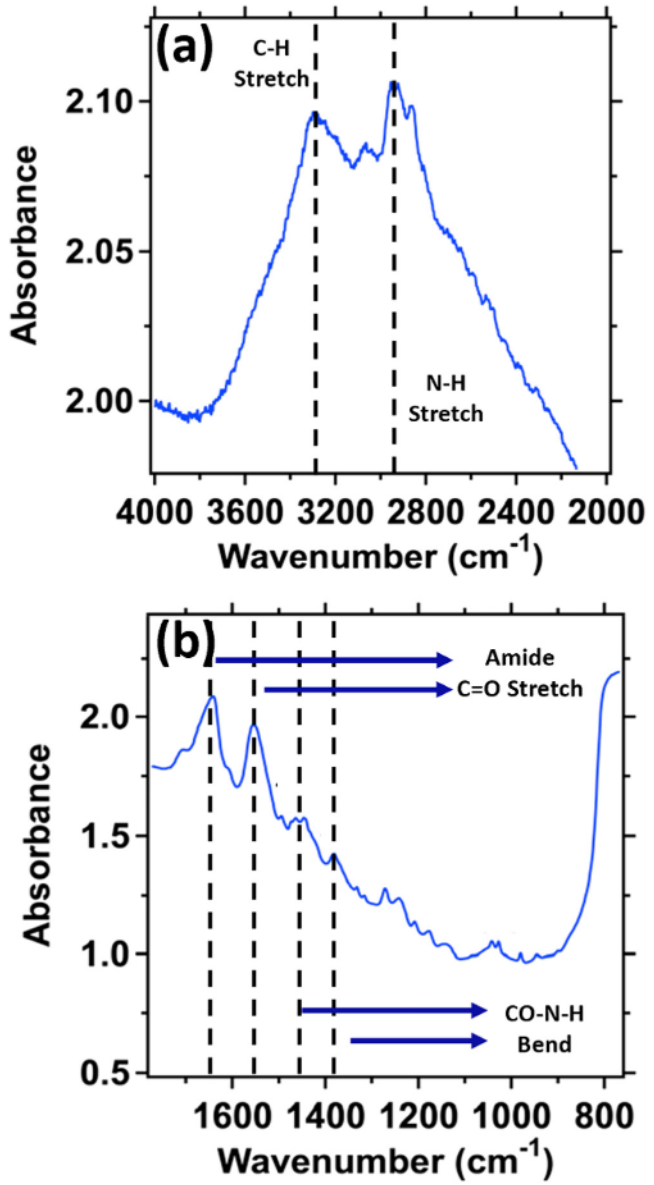

FIG. 11. FTIR spectra after 30 cycles of Nylon 2,6 MLD on ZrO_2 nanoparticles showing (a) C—H and N—H stretching and (b) C═O and CO—N—H amide stretching absorbance modes.

FTIR spectroscopy was also performed to characterize the Nylon 2,6 MLD film. Figure 11 shows absorbance peaks after 30 cycles of Nylon 2,6 were deposited on ZrO_2 nanoparticles at 67 °C. Figure 11(a) shows absorbance peaks at 3290 and 2939 cm^{-1}. These peaks are assigned to the C—H and N—H stretches, respectively. Figure 11(b) shows lower-energy absorbance peaks characteristic of the amide linkage. The amide I band at 1641 cm^{-1} is derived from C═O stretching vibrations. The amide II band at 1552 cm^{-1} is mainly derived from the in-plane stretching of N—H and CO—N—H bending modes. There is also small absorbance observed at 1380 cm^{-1} that results from C—H in-plane bending vibrational modes. All peaks in the FTIR spectra are consistent with previous reports of polyamide MLD systems.[6,7]

EDS mapping was also performed to confirm the elemental composition of the polyamide after deposition on particles. Figure 12 shows an EDS map of a thick Nylon 2,6 MLD film on a molecular solid substrate. The initial powder had been coated with 40 cycles of Al_2O_3 ALD using TMA and H_2O at 100 °C before being coated by 80 cycles of Nylon 2,6 MLD. Distinguishing the organic MLD film from the organic substrate is easier with the thin Al_2O_3 ALD layer in between the two organic materials.

The Nylon 2,6 film is evidenced by the C, O, N, and Cl signals in Fig. 12 in the top portion of the trilayer. These signals are consistent with the XPS spectrum displayed in Fig. 6. The chlorine concentration was measured to be only 0.9 at. %. This chlorine concentration is close to the chlorine contamination observed in the Nylon 2,6 MLD films on flat substrates. There is little to no mixing of the MLD and ALD layers as monitored by the clear definition between the two films at the interface depicted by the Al signal. Mixing is not expected when depositing organic films on an inorganic ALD coating. However, mixing can occur when depositing ALD coatings on organic substrates, as evidenced by a small nitrogen concentration in the Al_2O_3 ALD film.

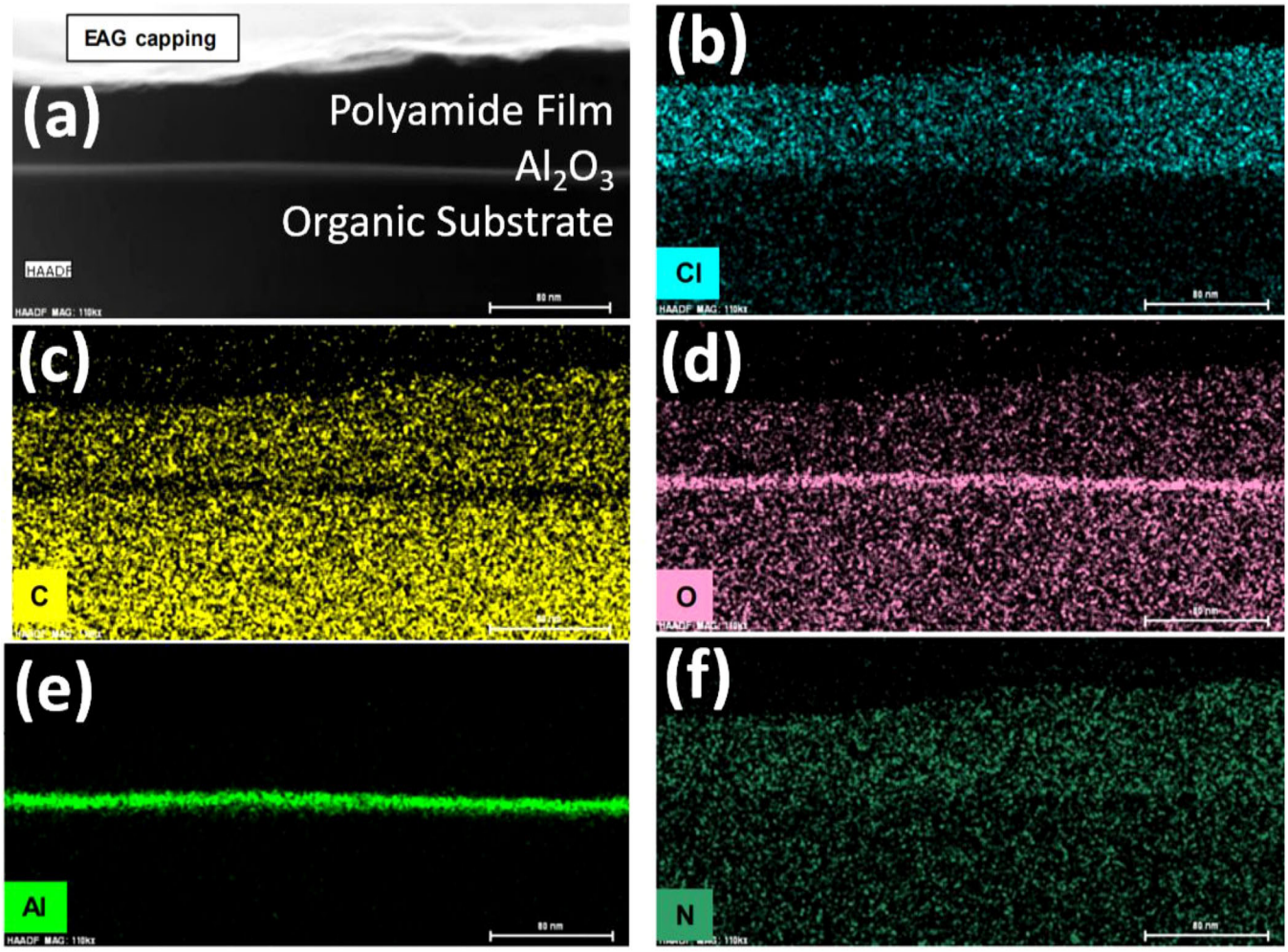

FIG. 12. Elemental map of (a) Nylon 2,6 MLD film deposited at 67 °C on a molecular solid previously coated with Al_2O_3 from the EDS signal of (b) Cl, (c) C, (d) O, (e) Al, and (f) N.

IV. CONCLUSIONS

Nylon 2,6 MLD was demonstrated at low temperatures using an isothermal enclosure containing a rotary reactor. The Nylon 2,6 polymer was deposited using MLD with adipoyl chloride and ethylene diamine as the homobifunctional MLD precursors. Growth of the Nylon 2,6 MLD polymer was investigated on both flat and powder substrates. XRR and SE measurements on flat substrates observed growth of the polymer over a range of temperatures with a peak growth rate of 4.0 Å/cycle at 67 °C. The growth was linear and showed lower growth rates at temperatures both above and below 67 °C. The growth rate was negligible at temperatures below 50 °C. The slower growth rate was attributed to short surface residence times at high temperatures and inadequate thermal activation at low temperatures.

The Nylon 2,6 MLD films grew conformally on ZrO_2, cellulose and metformin particle substrates. The MLD growth was consistent over particle sizes ranging from 10s of nanometers to 100s of micrometers. TEM images showed conformal films on the particles with thicknesses in agreement with the growth rates measured on flat substrates. The film thickness could also be controlled on particle substrates by varying the number of MLD cycles. The composition of the Nylon 2,6 film was determined on ZrO_2 witness wafers and powder substrates using FTIR, XPS, and EDS analyses. XPS and EDS observed C, N, and O with atomic percentages consistent with the expected composition of the Nylon 2,6 film. Only a small amount of chlorine contamination was observed in the films. FTIR analysis revealed the vibrational modes expected for a polyamide MLD film. The Nylon 2,6 MLD should be useful for

applications that require low-temperature MLD of all-organic polyamide films on flat and particle substrates.

ACKNOWLEDGMENTS

This research was supported by Applied Materials. The authors thank Andrew Cavanagh and Austin Cano for XPS and FTIR spectroscopy results. The authors also acknowledge EAG Laboratories for the EDS measurements. In addition, the authors thank Jim Kastengren and Don David of the Integrated Instrument Development Facility at the University of Colorado for their help in designing and machining parts for the isothermal enclosure and the rotary reactor.

DATA AVAILABILITY

The data that support the findings of this study are available within the article.

REFERENCES

[1]S. M. George, Chem. Rev. **110**, 111 (2010).
[2]V. Miikkulainen, M. Leskelä, M. Ritala, and R. L. Puurunen, J. Appl. Phys. **113**, 021301 (2013).
[3]S. M. George, B. Yoon, and A. A. Dameron, Acc. Chem. Res. **42**, 498 (2009).
[4]T. Yoshimura, S. Tatsuura, and W. Sotoyama, Appl. Phys. Lett. **59**, 482 (1991).
[5]P. Sundberg and M. Karppinen, Beilstein J. Nanotechnol. **5**, 1104 (2014).
[6]N. M. Adamczyk, A. A. Dameron, and S. M. George, Langmuir **24**, 2081 (2008).
[7]Y. Du and S. M. George, J. Phys. Chem. C **111**, 8509 (2007).
[8]D. J. Higgs, J. W. DuMont, K. Sharma, and S. M. George, J. Vac. Sci. Technol. A **36**, 01a117 (2018).
[9]J. M. Wallas *et al.*, ACS Appl. Energy Mater. **2**, 4135 (2019).
[10]B. C. Welch, O. M. McIntee, A. B. Ode, B. B. McKenzie, A. R. Greenberg, V. M. Bright, and S. M. George, J. Vac. Sci. Technol. A **38**, 052409 (2020).
[11]M. Junige and S. M. George, J. Vac. Sci. Technol. A **39**, 023204 (2021).
[12]M. Putkonen, J. Harjuoja, T. Sajavaara, and L. Niinistö, J. Mater. Chem. **17**, 664 (2007).
[13]A. Kim, M. A. Filler, S. Kim, and S. F. Bent, J. Am. Chem. Soc. **127**, 6123 (2005).
[14]P. W. Loscutoff, H. B. R. Lee, and S. F. Bent, Chem. Mater. **22**, 5563 (2010).
[15]J. S. Lee, Y. J. Lee, E. L. Tae, Y. S. Park, and K. B. Yoon, Science **301**, 818 (2003).
[16]T. V. Ivanova, P. S. Maydannik, and D. C. Cameron, J. Vac. Sci. Technol. A **30**, 01a121 (2012).
[17]T. Yoshimura, R. Ebihara, and A. Oshima, J. Vac. Sci. Technol. A **29**, 051510 (2011).
[18]A. Kubono and N. Okui, Prog. Polym. Sci. **19**, 389 (1994).
[19]J. R. Salem, F. O. Sequeda, J. Duran, W. Y. Lee, and R. M. Yang, J. Vac. Sci. Technol. A **4**, 369 (1986).
[20]Y. Takahashi, M. Iijima, K. Inagawa, and A. Itoh, J. Vac. Sci. Technol. A **5**, 2253 (1987).
[21]A. Kubono, N. Okui, K. Tanaka, S. Umemoto, and T. Sakai, Thin Solid Films **199**, 385 (1991).
[22]T. Miyamae, K. Tsukagoshi, O. Matsuoka, S. Yamamoto, and H. Nozoye, Jpn. J. Appl. Phys. **41**, 746 (2002).
[23]H. I. Shao, S. Umemoto, T. Kikutani, and N. Okui, Polymer **38**, 459 (1997).
[24]A. A. Dameron, D. Seghete, B. B. Burton, S. D. Davidson, A. S. Cavanagh, J. A. Bertrand, and S. M. George, Chem. Mater. **20**, 3315 (2008).
[25]Q. Peng, B. Gong, R. M. VanGundy, and G. N. Parsons, Chem. Mater. **21**, 820 (2009).
[26]B. Yoon, J. L. O'Patchen, D. Seghete, A. S. Cavanagh, and S. M. George, Chem. Vap. Depos. **15**, 112 (2009).
[27]B. H. Lee, V. R. Anderson, and S. M. George, Chem. Vap. Depos. **19**, 204 (2013).
[28]A. I. Abdulagatov, R. A. Hall, J. L. Sutherland, B. H. Lee, A. S. Cavanagh, and S. M. George, Chem. Mater. **24**, 2854 (2012).
[29]B. H. Lee, V. R. Anderson, and S. M. George, ACS Appl. Mater. Interfaces **6**, 16880 (2014).
[30]F. Caruso, Adv. Mater. **13**, 11 (2001).
[31]D. M. King, X. H. Liang, and A. W. Weimer, Powder Technol. **221**, 13 (2012).
[32]A. W. Weimer, J. Nanopart. Res. **21**, 9 (2019).
[33]J. D. Ferguson, A. W. Weimer, and S. M. George, Thin Solid Films **371**, 95 (2000).
[34]J. R. Wank, S. M. George, and A. W. Weimer, Powder Technol. **142**, 59 (2004).
[35]D. M. King, X. H. Liang, C. S. Carney, L. F. Hakim, P. Li, and A. W. Weimer, Adv. Funct. Mater. **18**, 607 (2008).
[36]D. M. King, X. H. Liang, P. Li, and A. W. Weimer, Thin Solid Films **516**, 8517 (2008).
[37]D. M. King, X. H. Liang, B. B. Burton, M. K. Akhtar, and A. W. Weimer, Nanotechnology **19**, 255604 (2008).
[38]L. F. Hakim, S. M. George, and A. W. Weimer, Nanotechnology **16**, S375 (2005).
[39]J. D. Ferguson, K. J. Buechler, A. W. Weimer, and S. M. George, Powder Technol. **156**, 154 (2005).
[40]J. D. Ferguson, A. W. Weimer, and S. M. George, Chem. Mater. **16**, 5602 (2004).
[41]A. S. Cavanagh, C. A. Wilson, A. W. Weimer, and S. M. George, Nanotechnology **20**, 255602 (2009).
[42]C. F. Herrmann, F. H. Fabreguette, D. S. Finch, R. Geiss, and S. M. George, Appl. Phys. Lett. **87**, 123110 (2005).
[43]Y. S. Jung, A. S. Cavanagh, A. C. Dillon, M. D. Groner, S. M. George, and S. H. Lee, J. Electrochem. Soc. **157**, A75 (2010).
[44]Y. S. Jung, A. S. Cavanagh, L. A. Riley, S. H. Kang, A. C. Dillon, M. D. Groner, S. M. George, and S. H. Lee, Adv. Mater. **22**, 2172 (2010).
[45]X. B. Meng, X. Q. Yang, and X. L. Sun, Adv. Mater. **24**, 3589 (2012).
[46]S. Vajda *et al.*, Nat. Mater. **8**, 213 (2009).
[47]Y. Zhou, D. M. King, X. H. Liang, J. H. Li, and A. W. Weimer, Appl. Catal. B **101**, 54 (2010).
[48]X. Liang, D. M. King, P. Li, S. M. George, and A. W. Weimer, AlChE J. **55**, 1030 (2009).
[49]X. H. Liang, Y. B. Jiang, and A. W. Weimer, J. Vac. Sci. Technol. A **30**, 01a108 (2012).
[50]R. L. Patel, Y. B. Jiang, and X. H. Liang, Ceram. Int. **41**, 2240 (2015).
[51]D. M. Piper, J. J. Travis, M. Young, S. B. Son, S. C. Kim, K. H. Oh, S. M. George, C. M. Ban, and S. H. Lee, Adv. Mater. **26**, 1596 (2014).
[52]T. D. Gould, A. Izar, A. W. Weimer, J. L. Falconer, and J. W. Medlin, ACS Catal. **4**, 2714 (2014).
[53]X. H. Liang, M. Yu, J. H. Li, Y. B. Jiang, and A. W. Weimer, Chem. Commun. **46**, 7140 (2009).
[54]L. J. Qin, N. Yan, H. X. Hao, T. An, F. Q. Zhao, and H. Feng, Appl. Surf. Sci. **436**, 548 (2018).
[55]S. A. Vasudevan, Y. L. Xu, S. Karwal, H. van Ostaay, G. M. H. Meesters, M. Talebi, E. J. R. Sudhölter, and J. R. van Ommen, Chem. Commun. **51**, 12540 (2015).
[56]J. A. McCormick, B. L. Cloutier, A. W. Weimer, and S. M. George, J. Vac. Sci. Technol. A **25**, 67 (2007).
[57]J. W. Clancey, A. S. Cavanagh, R. S. Kukreja, A. Kongkanand, and S. M. George, J. Vac. Sci. Technol. A **33**, 01a130 (2015).
[58]D. Longrie, D. Deduytsche, and C. Detavernier, J. Vac. Sci. Technol. A **32**, 010802 (2014).
[59]K. Kawakami, Pharmaceutics **11**, 202 (2019).
[60]D. Seghete, R. A. Hall, B. Yoon, and S. M. George, Langmuir **26**, 19045 (2010).
[61]C. A. Wilson, R. K. Grubbs, and S. M. George, Chem. Mater. **17**, 5625 (2005).